



Bulk Nanostructured Extruded Material Based on $\text{Bi}_2\text{Te}_{2.7}\text{Se}_{0.3}$ Solid Solution for Thermoelectric Converters

Tagiyev M.M.^{1*}, Nagiyev T.G.¹, Abdinova G.D.², Aliyev R.Y.²,
Magerramova K.I., Pirieva T.I.²

¹Azerbaijan State Economic University, AZ1001 Baku, Azerbaijan

²Institute of Physics of the Ministry of Science and Education of Azerbaijan AZ1141 Baku,
Azerbaijan

mail_tagiyev@mail.ru

Abstract. The electrical properties of extruded bulk nanostructured samples of the $\text{Bi}_2\text{Te}_{2.7}\text{Se}_{0.3}$ solid solution were studied in the temperature range of 77–300 K and magnetic field strength up to 74×10^4 A/m that did not undergo annealing after extrusion, and the same samples that underwent optimal annealing. It was found that at low temperatures, charge carriers are primarily scattered by structural defects and grain boundaries. As grain size increases, the number of grain boundaries and the concentration of defects within grains decrease. As grain size increases, the concentration due to ionized defects decreases, leading to increased charge carrier mobility.

Keywords: grain, nanostructure, extrusion. mobility, defects.

1. Introduction

Thermoelectric cooling using semiconductor materials is currently receiving considerable attention. This new branch of modern technology offers a fundamentally new approach to creating compact devices for reducing and stabilizing temperatures in localized volumes. Thermoelectric cooling is the best technical solution for cooling and thermally stabilizing heat-generating elements in electronic and optical devices [1-4]. The best materials for thermoelement legs are Bi_2Te_3 - Bi_2Se_3 (n-type conductivity) and Bi_2Te_3 - Sb_2Te_3 (p-type conductivity) solid solutions. Due to the increasing demand for thermoelements, the development of new high-performance methods for obtaining thermoelement legs is a very pressing issue. Undoubtedly, of particular interest is the creation of nanothermoelectrics that allow their mass production. Currently, one of the cheapest technologies is the creation of bulk nanostructured materials by mechanical activation treatment in ball mills followed by hot pressing [5,6]. An increase in the quality factor when using nanostructures can be achieved by the following mechanisms: additional phonon scattering at the boundaries of nanograins; electron tunneling between nanostructural elements; energy filtration of carriers due to the presence of potential barriers between nanograins. In this paper, we discuss the mechanisms for increasing the thermoelectric figure of merit and study the effect of nanograin size on the magnitude of the kinetic coefficients in $\text{Bi}_2\text{Te}_{2.7}\text{Se}_{0.3}$ materials.

© The Author(s) 2026

R. Rzayev et al. (eds.), *Proceedings of the International Conference on Current Problems in Engineering and Applied Sciences (ICCPEAS 2025)*, Advances in Engineering Research 299,

https://doi.org/10.2991/978-94-6239-668-5_14

Single crystals of the $\text{Bi}_2\text{Te}_{2.7}\text{Se}_{0.3}$ solid solution are efficient n-type thermoelectric materials and are recommended for use in energy converters at temperatures of $\sim 200\div 300\text{K}$. However, due to its layered structure, this material is severely damaged during the fabrication of thermoelement legs and the assembly of thermoelectric energy converters based on them, resulting in an exceptionally low yield. At the same time, the low mechanical strength of single crystals, due to their structural features, reduces the reliability of energy converters under critical conditions. Thermoelectric material produced by extrusion, which is a fine-grained polycrystal, exhibits higher mechanical strength and thermoelectric parameters close to those of single crystals. Thermoelectrics based on Bi-Sb-Te-Se solid solutions exhibit the highest figure of merit at moderate temperatures. Therefore, these materials are of interest for enhancing their thermoelectric figure of merit (Z) through nanostructuring. Methods for increasing the efficiency of thermoelectric materials boil down to the creation of structural defects that can influence, to varying degrees, the scattering of charge carriers and phonons. In recent years, suggestions have been made regarding the possibility of increasing Z in materials with two-dimensional and three-dimensional defects in the crystal structure, the distances between which are comparable to the mean free path of charge carriers or the wavelength of acoustic phonons responsible for heat transfer. These suggestions are based on the possibility of creating conditions under which, in areas of the material with different physical properties, stronger scattering of thermal vibrations occurs than that of electrons and holes. In a highly porous dispersed system, the surface layers of particles can have a significant influence on Z . Dispersion leads to the appearance of numerous defects on the surface of the grains that make up the heterogeneous system [7].

There is a potential for a preferential reduction in thermal conductivity due to grain-boundary phonon scattering due to changes in their phase velocity at grain boundaries. The phase velocity of charge carriers also changes at grain boundaries, and the change in thermoelectric efficiency is determined by the ratio of additional electron and phonon scattering processes.

The existence of a developed system of grain and subgrain boundaries in a material can lead to an increase in its efficiency if either charge carriers or phonons are predominantly scattered at the boundaries. Currently, uniaxial compression of n- and p-type bismuth telluride crystals is used to increase thermoelectric efficiency; this leads to an increase in the material's quality factor due to a change in the power factor ($\alpha^2\sigma$) [8].

The miniaturization of electronic coolers is becoming increasingly important. This requires the production of thermoelement legs of a size comparable to the depth of the single-crystal thermoelectric material layer damaged during cutting into the legs. This significantly reduces the actual thermoelectric efficiency of the thermoelectric energy converter. The highest thermoelectric figure of merit at moderate temperatures (below $\sim 300\text{K}$) is found in $\text{Bi}_2\text{Te}_{2.7}\text{Se}_{0.3}$ solid solution samples with grain sizes of $\sim 630\ \mu\text{m}$ [9]. Therefore, these compositions are of particular interest from the standpoint of the potential for enhancing their thermoelectric properties through nanostructuring. In order to study the influence of nanostructuring on the phenomenon of heat and charge transfer in extruded samples of the $\text{Bi}_2\text{Te}_{2.7}\text{Se}_{0.3}$ solid solution,

the electrical properties of extruded bulk nanostructured samples of the Bi₂Te_{2.7}Se_{0.3} solid solution were obtained and studied in the temperature range of $\sim 77\div 300$ K and magnetic field strength up to $\sim 74 \times 10^4$ A/m, on samples that did not undergo annealing after extrusion, and on the same samples that underwent optimal annealing.

2. Experimental Part

High-purity bismuth (VI-0000) was used to obtain the studied samples. Se (for rectifiers) and tellurium were of chemically pure grade, and distilled (or doubly sublimed) tellurium of special purity (T-Schl) was used.

Synthesis was performed by direct alloying of the components. The starting materials were placed in a stoichiometric ratio in a quartz ampoule, pre-etched in a solution of bichromate ($\text{K}_2\text{Cr}_2\text{O}_7 + \text{H}_2\text{SO}_4$) and rinsed with distilled water. The ampoule was evacuated to a residual pressure of 10^{-3} Pa and sealed off. Synthesis was carried out at a temperature of $\sim 1053 \text{ K} \pm 5 \text{ K}$ for 2 hours. To improve alloy homogeneity, the ampoule containing the melt was shaken using a special device. The material was then cooled to room temperature by immersion in water.

The semiconductor material (SPM) was ground in a porcelain cup, and a fraction with a particle size of ≤ 0.1 mm was collected. Nanosized powders were obtained from Bi₂Te_{2.7}Se_{0.3} powders with a particle size of ≤ 0.1 mm using an AGO-2 ball mill. An XRD D8 ADVANCE X-ray system (Bruker, Germany) and TOPAS-4.2 and EVA software were used to determine the particle size in the powder. The nanoparticle sizes were determined and had dimensions of 1.6×10^5 ; 38; 30 and 15 nm.

The crushed semiconductor material was pressed into blanks (briquettes) at a temperature of $\sim 300 \text{ K}$ and a pressure of 450 MPa. The briquettes had a diameter of approximately 30 mm.

The specimens (thermoelement legs) were formed by extrusion. The extrusion process conditions (temperature, pressure, draw ratio, etc.) significantly affect the material's properties and the homogeneity of their distribution, as well as the mechanism and kinetics of the processes occurring during post-extrusion annealing of the material. A favorable combination of process parameters allows extrusion to produce rods free of macroscopic defects, with uniform thermoelectric and mechanical properties, and high thermoelectric and mechanical properties.

Extrusion was performed on an MS-1000 hydraulic press from a diameter of 30 mm to a diameter of 6 mm (drawing ratio -25).

Extrusion process parameters:

Extrusion temperature - $T_{\text{ex}} = 653 \pm 3 \text{ K}$,

Extrusion pressure - $P_{\text{ex}} = 9 \text{ t/cm}^2$

Hot briquetting (extrusion) produces a high-density material without delamination cracks.

Post-extrusion annealing was performed in quartz ampoules at $\sim 690 \text{ K}$ for 5 hours at 10^{-3} Pa evacuated pressure.

Cutting of the cylindrical sample into parallelepiped-shaped specimens was performed using an A207.40M electrical discharge machine. When cutting crystals of bismuth telluride-based solid solutions, a damaged layer with properties and structure

different from the rest of the material appears on the cut surface, significantly reducing their thermoelectric figure of merit. A thickness of $10\div 15\ \mu\text{m}$ formed during cutting was removed from the sample surface by electrochemical etching. The depth of the damaged layer was estimated from the time dependence of the etching rate, which differs for deformed and undeformed material. Removing the damaged layer improved the parameters of the studied specimens.

The etching rate of grains in a large-block aggregate depends on their orientation relative to the cutting plane and varies for different grains. In fine-grained polycrystalline material obtained by the Bridgman method, the etching rate is averaged over orientations in [10]. The nature of the structure of the damaged layer was investigated radiographically by imaging a stationary sample in reflection to an RKSO chamber, using radiation from a tube with copper anticatalytic agents; the depth of the semi-absorbing layer was $\sim 15\ \mu\text{m}$.

X-ray texture analysis was carried out on nanostructured $\text{Bi}_2\text{Te}_{2.7}\text{Se}_{0.3}$ samples with different grain sizes. To study the texture, the intensity of reflections (0006) and (1120) from three or five sections of the rods was analyzed. The sections were made at angles of 0° ; 180° ; 360° ; 540° 720° or 0° ; 450° ; 90° to the extrusion axis. The survey was carried out on a diffractometer with monochromatic radiation of a tube with an iron anode at a primary beam divergence of no more than 1° and an inclination relative to the horizontal axis of the goniometer with a step of 2° . For the studied samples, tilting the working surface relative to the goniometer axis by more than $25\text{-}30$ degrees is undesirable due to severe defocusing. A correction for defocusing due to tilt was introduced based on the results of surveying the sample with the working surface parallel to the extrusion axis, while rotating it around the extrusion axis. The angular intensity distribution obtained when surveying different sections was stitched together using common points. Thus, the dependence of the beam intensity on the tilt angle of the reflecting planes diffracted relative to the extrusion axis was studied in the angular range $\varphi = 0 \div 90^\circ$ with a step of 20° . The determination of the orientation probability density function ρ_φ from the experimental values of the angular intensity distribution was carried out using the formula

$$\rho_{\varphi,\psi} = \frac{2}{3} [\rho_{\varphi,\psi}]^3 \Delta\varphi \Delta\psi \sin \varphi$$

A high-speed digital universal measuring instrument (TsUIP) with an accuracy class of 0.02 and high input impedance was used as the recording device, allowing for high-precision recording of measured values. The linear dimensions of the samples were monitored using an MBS-1 microscope with an accuracy class of 0.005 mm.

The bending strength of the obtained bulk nanostructured samples of $\text{Bi}_2\text{Te}_{2.7}\text{Se}_{0.3}$ using the method described in [11] and it was found that the strength of these samples is ~ 3 times higher than the strength of single-crystal samples.

Electrical conductivity (σ), thermoelectric power (α) and the Hall effect (R_H) were measured using a stationary potentiometric method [12].

The electrical parameters of the studied samples of the sample length (rod), i.e. in the direction of extrusion, were measured along.

The error in measuring electrical parameters did not exceed $\pm 3\%$.

3. Results and discussion

The results obtained are presented in Figs. 1 and 2 and the table 1. It is evident that heat treatment has different effects on the electrical properties of the studied samples with different grain sizes. A significant change is observed in samples with a minimum grain size of 15 nm.

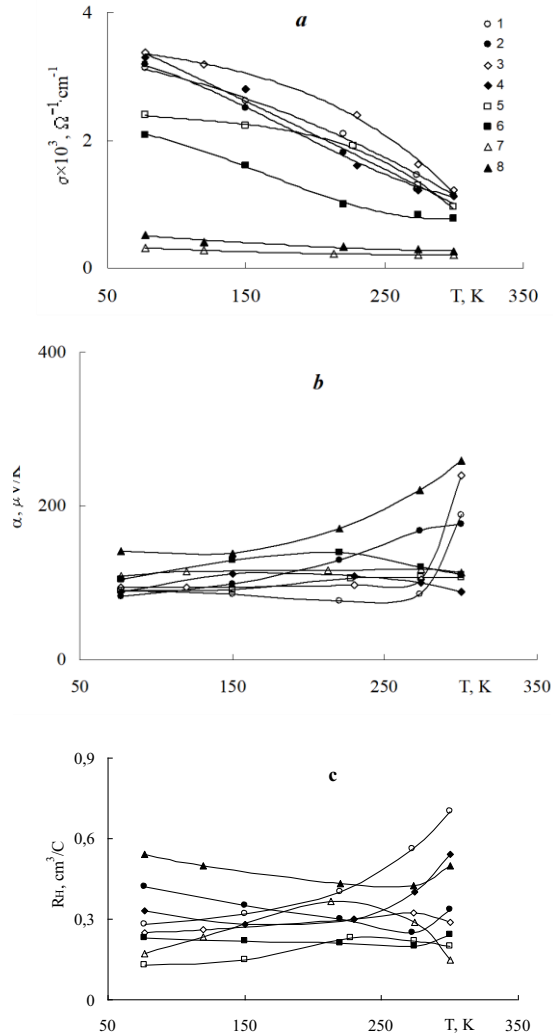


Fig.1. Dependence of electrical conductivity σ (a), Seebeck coefficient α (b) and Hall coefficient R_h (c) on temperature of extruded samples of Bi₂Te_{2.7}Se_{0.3} solid solution with different grain sizes. Curves refer: 1 and 2 for samples of 1.6×10^5 nm; 3 and 4 for samples of 38 nm; 5 and 6 for samples of 30 nm; 7 and 8 for samples of 15 nm. 1, 3, 5 and 7 are unannealed samples, 2, 4, 6 and 8 are annealed samples.

The temperature dependence of the Seebeck coefficient indicates that the materials under study are not highly degenerate: $(d|S|/dT)$ corresponds to that found in single crystals with increasing close compositions and has a tendency to decrease the electron concentration at $\sim 77\text{K}$. Nanostructuring does not change the temperature dependence of electrical conductivity, which in the studied temperature range is described by the acoustic scattering mechanism for unannealed samples. Electrical conductivity decreases with increasing temperature for all samples, i.e., for both annealed and unannealed samples, which is associated with a change in the drift mobility of electrons.

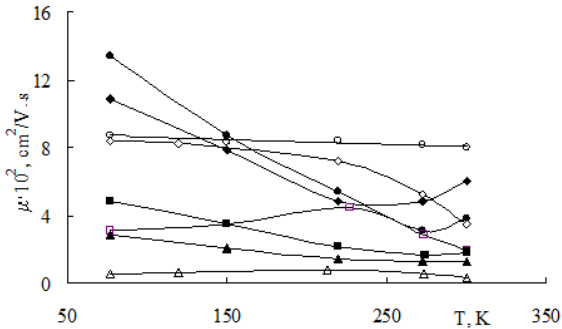


Fig. 2. Dependence of the Hall mobility μ on the temperature of extruded samples of the $\text{Bi}_2\text{Te}_{2.7}\text{Se}_{0.3}$ solid solution with different grain sizes. Designations are the same as in Fig.1

In the high-temperature region, the coefficient β as a function $\sigma \sim T^\beta$ is close to the data in [13].

Deformation during extrusion of polycrystalline materials based on Bi_2Te_3 leads to the formation of two types of texture in the rod: axial /110/ and ring (001); the existence of a non-textured material is possible. The ratio of the quantities and the degree of perfection of the texture components depends on many factors: in composite materials, on the type and quantity of the modifying additive, the base material, the temperature regime of extrusion and post-extrusion annealing [3].

Axial /110/ and ring (001) textures are favorable for thermoelectric properties; the basal planes of crystals (planes of increased mobility) are located along the rod axis.

The textures formed as a result of plastic flow of the material are determined by which slip systems are activated and what is the contribution of grain boundary deformation (deformation pattern, temperature, speed, structure of the workpiece, and under conditions of dynamic recrystallization - the degree of recrystallization).

An analysis of deformation and post-deformation annealing textures in tetradymites is aimed at quantifying the probability of basal plane coincidence with the extrusion axis and assessing the contribution of each grain to the macroscopic conductivity along the rod axis. The mechanism of texture formation (basal slip, multiple slip) is also important, as different textures are characterized by different substructures.

tures (and components can therefore have different microconductivity) and varying levels of chemical homogeneity in the distribution of base material components.

For example, if tellurium complexes represent interquintet formations, then basal sliding cannot lead to their destruction.

In the studied samples, extrusion, in which the deformation pattern is similar to uniaxial tension, leads to the formation of axisymmetric orientations. In this case, the pole density distribution is characterized by a body of revolution with an axis parallel to the direction of the external force.

Table 1. Electrical parameters of extruded bulk nanostructured samples of the Bi₂Te_{2.7}Se_{0.3} solid solution.

Grain size (nm)	Before annealing									
	77K					300K				
	$\sigma, \Omega^{-1} \text{cm}^{-1}$	$\alpha, \mu\text{V/K}$	$R_{H1}, \text{cm}^3/\text{C}$	$\mu, \text{cm}^2/\text{V}\cdot\text{s}$	$n \times 10^{19}, \text{cm}^{-3}$	$\sigma, \Omega^{-1} \text{cm}^{-1}$	$\alpha, \mu\text{V/K}$	$R_{H1}, \text{cm}^3/\text{C}$	$\mu, \text{cm}^2/\text{V}\cdot\text{s}$	$n \times 10^{19}, \text{cm}^{-3}$
1.6×10^3	3125	90	0.28	875	2.23	1145	88	0.7	802	8.92
38	3369	94	0.25	842	2.5	1219	240	0.27	329	2.31
30	2394	90	0.13	311	4.81	950	107	0.2	190	3.13
15	314	109	0.17	53	3.18	208	113	0.15	31	4.17
After annealing										
1.6×10^3	3180	83	0.42	1336	1.48	1141	176	0.64	859	7.44
38	3292	89	0.33	1086	1.89	1117	88	0.54	603	1.16
30	2087	104	0.23	480	2.72	766	111	0.27	207	2.31
15	521	141	0.54	281	1.16	255	259	0.5	128	1.25

Specific electrical conductivity decreases monotonically with temperature and increases with increasing grain size. For all studied samples, below ~ 200 K, the temperature dependences of μ and α are typical for the impurity conductivity region.

The Seebeck coefficient for all samples with nanosized grains increases with temperature for both annealed and unannealed samples. The deviation of the $\alpha(T)$ dependence from the linear B temperature region above ~ 270 K is assumed to be due to the onset of intrinsic conductivity. Due to the fine-crystalline structure of the extruded samples of the Bi₂Te_{2.7}Se_{0.3} solid solution, the mean free path, determined by standard formulas for the parabolic zone and acoustic scattering [14], is smaller than the grain size.

The presence of potential barriers between different grains in bulk nanostructures can lead to a strong energy dependence of the mean free path of charge carriers near the chemical potential level. This results in carrier filtering, whereby carriers with energies above the Fermi energy will cross the grain boundary without scattering.

As a result of experimental studies and theoretical analysis, it was found that it is advisable to use semiconductors with high mobility of most charge carriers, large effective mass and low lattice thermal conductivity as thermoelectric materials.

$$Z \sim \left(\frac{\mu}{\chi_l} \right) \cdot \left(\frac{m^*}{m_0} \right)^{3/2} \cdot T^{3/2}$$

Where μ - is the drift mobility of charge carriers;

χ_l -is the lattice component of thermal conductivity;

m_0 - is the mass of a free electron;
 m^* - is the effective mass of charge carriers;
 T - is the absolute temperature.

The analysis of the dependence of R_x on the orientation of the field and the direction of the current relative to the extrusion axis showed that R_x of the polycrystalline extruded sample is isotropic, and the calculated Hall mobilities of charge carriers at $T=\text{const}$ correlate with the parameter $\mu_0(m^*/m_0)^{3/2}$,

Where- μ_0 is the carrier drift mobility in the absence of degeneracy;

$m^* \sim T^s$ ($s=0.12$; 0.14 for Bi_2Te_3 n- and p-type conductivity, respectively). The dependence of the effective mass on temperature was confirmed experimentally [16]. Thus, micromobility can be judged using the parameter $\mu_0(m^*/m_0)^{3/2}$, for the determination of which it is sufficient to measure the electrical conductivity in two directions and the thermo-emf coefficient, which is isotropic to within experimental error.

Calculation of the Hall mobility based on experimental values of electrical conductivity and the Hall coefficient revealed that, in all samples, both heat-treated and unheat-treated, it increases with increasing grain size across the entire temperature range studied. The most pronounced change during heat treatment is observed in samples with the smallest grain sizes (Table). The mobility of the heat-treated samples exceeds that of the unheat-treated samples. Charge carrier mobility is determined by scattering from deformation-induced structural defects.

When calculating the charge carrier mobility and electrical conductivity taking into account scattering at grain boundaries under the assumption that the main scattering mechanism is scattering by acoustic phonons. For Bi_2Te_3 and its analogs in a wide range of temperatures and concentrations, $r = -0.5$. For thermoelectric applications, an important parameter [17].

$$\mu_0 \left(\frac{m^*}{m_0} \right)^{3/2} = \frac{\sigma_r (r+1,5)}{2l(2\pi m_0 k_0 T/h^2 \cdot F_{r+0,5}(\xi^*))}$$

μ_0 - is the drift mobility of charge carriers in the absence of degeneracy;

k_0 - is the Boltzmann constant;

h - is Planck's constant;

$E^* = E/kT$, E - is the chemical potential of free charge carriers.

$\xi^* = \xi/k_0T$

ξ - chemical potential of free charge carriers,

counted positively from the bottom of the conduction band for electrons and downwards from the top of the valence band for holes, for

F , - taken from [18].

For degenerate samples, the Seebeck coefficient is described by the expression

$$|\alpha| = \frac{k_0}{e} \left\{ \frac{(2r+5)F_{r+1,5}(\xi^*)}{(2r+3)F_{r+0,5}(\xi^*)} - \xi \right\}$$

The decrease in electrical conductivity with increasing temperature in all samples is associated with a decrease in the drift mobility of charge carriers $\mu = \mu_0 T^b$ and the resonant potential. This change in mobility is due to the simultaneous scattering of carri-

ers on the optical and acoustic deformation potential. With a decrease in electrical conductivity, the dependence $\sigma = f(T)$ decreases.

During extrusion, the grains of the crystals of the material being studied change their orientation and axial shape relative to the deforming forces (in the direction of the extrusion axis). At high degrees of deformation, a texture is formed, which causes the formation of a recrystallization texture and, simultaneously, various electroactive structural defects. In this case, the newly recrystallized grains have a crystallographic orientation. The nature and degree of texture are primarily determined by grain size, the temperature of the post-extrusion annealing, etc. At low annealing temperatures, recrystallization is the same as the deformation texture. At high annealing temperatures, the recrystallization texture often differs from the deformation texture or is absent. Defects created during plastic deformation serve as scattering centers for charge carriers, reducing their mobility. As crystallite (grain) size decreases, the energy required for grain orientation simultaneously decreases, leading to an increase in the degree of texture in the sample. Samples with minimal grain sizes exhibit high carrier concentrations due to the highly dispersed nature of the medium. In samples with larger grain sizes, the energy required for grain orientation, i.e., the energy required for texture formation, simultaneously increases. Heat treatment "heals" structural defects, normalizing the structure of the studied samples. Annealing leads to structural normalization, leading to increased mobility and, simultaneously, to decrease in the degree of texture, which is explained by the disorientation of grains due to thermal energy. The influence of grain orientation varies for different ratios of geometric dimensions of thermoelements made from these samples.

Thus, in bulk nanostructured samples that have not undergone annealing, at low temperatures, charge carriers are primarily scattered by structural defects and grain boundaries. As grain size increases, the number of grain boundaries and the concentration of defects within the grains decrease. Due to the increase in grain size, the concentration due to ionized defects decreases, leading to increased charge carrier mobility within the sample.

It was found that nanostructuring and heat treatment in extruded samples of Bi₂Te_{2.7}Se_{0.3} does not change the temperature dependence of electrical conductivity, mobility and thermoelectric coefficient along the extrusion axis.

The value of $\mu_0(m^*/m_0)^{3/2}$ for a known scattering parameter in the region of impurity conductivity can be calculated from experimentally determined values of two measured parameters of electrical conductivity and the thermoelectric coefficient.

4. Conclusion

In nanostructured Bi₂Te_{2.7}Se_{0.3} samples annealed at low non-bulk temperatures, charge carriers are primarily scattered by structural defects and grain boundaries. With increasing grain size, the number of grain boundaries and the concentration of defects within the grains decrease. Due to the increase in grain size, the concentration due to ionized defects decreases, leading to an increase in charge carrier mobility in the sample. The decrease in electrical conductivity with increasing temperature in all samples is associated with a decrease in the drift mobility of charge carriers $\mu = \mu_0 T^\beta$. This change in mobility is due to the simultaneous scattering of carriers by the optical

and acoustic strain potentials. With a decrease in electrical conductivity, the dependence $\sigma = f(T)$ decreases.

Declaration

This is supported by the state budget of the Republic of Azerbaijan, and the experiments were conducted at the Institute of Physics, Ministry of Science and Education of Azerbaijan.

References

1. Ivanova L.D.: Thermoelectric materials for different temperature levels. *Solid state physics* 51(7), 909-912. doi: 10.1134/S1063782617070132 (2017)
2. Yapryntseva E.N., Ivanov O.N., Vasiliev A.E., Shukhova V.G.: Microstructure and thermoelectric properties of medium-entropy compounds BiSbTe 1.5Se1.5 PbSnTeSe obtained by reactive spark plasma sintering. *FTP* 2 141-144 (2022)
3. Kazimov M.V., Ibragimov G.B., Isakov G.I., Ibragimov B.G. : Physical-chemical properties of InSb+Mg₃Sb₂ eutectic systems: synthesis, characterization, and applications *Journal of Optoelectronic and Biomedical Materials* 14(4), 187-190 (2022)
4. Nemov S.A., Ulashkevich Yu.V., Rulimov A.A., Demchenko A.E., Allahhah A.A., Sveshnikov I.V., Dzhaferov M.: About the band structure of Bi₂Te₃. *FTP* 53(5), 608-611(2019)
5. Poduel B., Hao Qing., Ma Yi., Lan Yucheng., Minnich Austin., Yu Bo., Yan Xiao., Wang Dezhi., Muto Andrew., Vashae Daryoosh., Chen Xiaoyuan., Liu Junming., Dresselhaus Mildred S., Chen Gang., Ren Zhifeng.: *Science* 320 (5876), 634 -638. (2008)
6. Bulat L.P., Drabkin I.A., Karataev V.V., Osvensky V.B., Pshenai-Severin D.A.: On the thermoelectric figure of merit in bulk nanocrystals. *Thermoelectrics and their Applications* 41 (2010).
7. Volkenstein F.S. *Physical chemistry of semiconductor surfaces*. Moscow: Nauka (1973)
8. Bulat L.P., Drabkin I.A., Karataev V.V., Osvensky V.B., Pshenai-Severin D.A.:Effect of scattering at boundaries on the thermal conductivity of a nanostructured semiconductor material based on a solid solution Bi_xSb_{2-x}Te₃. *Solid state physics* 52(9) 1712-1716 (2010)
9. Barkhalov B.Sh., Tagiyev M.M., Bagieva G.Z.,Abdinova G.D., AlievR.Yu., K.I.Magerramova. : Influence of grain size on the thermoelectric properties of extruded samples of Bi_{0.5}Sb_{1.5}Te₃ solid solution *Izvestiya Universities* 62(4) 94-101 (2019)
10. Alieva T.D., Abdinov D.Sh., Salaev E.Yu.: Effect of surface treatment of thermoelectric materials on the properties of thermoelements made from solid solutions of the Bi₂Te₃-Bi₂Se₃ and Bi₂Te₃-Sb₂Te₃ systems *Izvestiya AN SSSR. Inorganic materials*. 17(10) 1773–1776 (1981)
11. Sidorenko N.A., Dashevsky Z.M. : Efficient Bi-Sb crystals for thermoelectric cooling at temperatures T≤180K *Semiconductors* 53(5) 693-697 (2019)

12. Ochotin A.S., Pushkarski A.S., Borovikova R.P., Simonov V.A. : Methods of measuring characteristics of thermoelectric materials and converters. Moscow Nauka. (1974)
13. Stark N.K., Svechnikova T.E., Chizhevskaya S.N. : Thermoelectric properties of Bi₂Te₃-Bi₂Se₃ system alloys in the temperature range of 100-600K Bulletin of the USSR Academy of Sciences. Inorganic materials. 21(3) 390-392 (1985)
14. Stilbans L.S. : Physics of Semiconductors. Moscow; Soviet Radio (1967)
15. Kireev P.S. : Physics of Semiconductors. Moscow; Higher School. (1975)
16. Dik M.G., Agaev Z.F., Dubrovina A.N., Abdinov D.Sh. : Effect of modification on hole mobility and thermal conductivity of extruded samples of solid solutions of the Bi₂Te₃-Sb₂Te₃ system Izvestiya AN SSSR. Inorganic materials 24(8)1290-1293 (1988)
17. Goltsman B.M., Kudinov V.A., Smirnov I.A.: Semiconductor thermoelectric materials based on Bi₂Te₃. Moscow: Nauka..320 (1972)
18. Blackmore J., : Statistics of Electrons in Semiconductors. Moscow: Mir, 375 (1964)

Open Access This chapter is licensed under the terms of the Creative Commons Attribution-NonCommercial 4.0 International License (<http://creativecommons.org/licenses/by-nc/4.0/>), which permits any noncommercial use, sharing, adaptation, distribution and reproduction in any medium or format, as long as you give appropriate credit to the original author(s) and the source, provide a link to the Creative Commons license and indicate if changes were made.

The images or other third party material in this chapter are included in the chapter's Creative Commons license, unless indicated otherwise in a credit line to the material. If material is not included in the chapter's Creative Commons license and your intended use is not permitted by statutory regulation or exceeds the permitted use, you will need to obtain permission directly from the copyright holder.

